Structural Engineering and Mechanics, Vol. 7, No. 4 (1999) 387-400
DOI: http://dx.doi.org/10.12989/sem.1999.7.4.387

Effect of excitation type on dynamic system parameters of a reinforced concrete bridge

M.M. Abdel Wahab†

Department of Mechanical and Materials Engineering, University of Surrey, Guildford, Surrey, GU2 5XH, U.K.

G. De Roeck‡

Department of Civil Engineering, Katholieke Universiteit te Leuven, 3001-Heverlee, Belgium

Abstract. Damage detection in civil engineering structures using the change in dynamic system parameters has gained a lot of scientific interest during the last decade. By repeating a dynamic test on a structure after a certain time of use, the change in modal parameters can be used to quantify and qualify damages. To be able to use the modal parameters confidentially for damage evaluation, the effect of other parameters such as excitation type, ambient conditions,... should be considered. In this paper, the influence of excitation type on the dynamic system parameters of a highway prestressed concrete bridge is investigated. The bridge, B13, lies between the villages Vilvoorde and Melsbroek and crosses the highway E19 between Brussels and Antwerpen in Belgium. A drop weight and ambient vibration are used to excite the bridge and the response at selected points is recorded. A finite element model is constructed to support and verify the dynamic measurements. It is found that the difference between the natural frequencies measured using impact weight and ambient vibration is in general less than 1%.

Key words: dynamic measurement on bridges; system identification; ambient/forced vibration.

1. Introduction

Due to the limitation of the classical visual inspection technique to detect damage in structures, damage evaluation by dynamic system identification has gained a lot of attention in the engineering community. The dynamic system parameters such as natural frequencies, damping ratios and mode shapes are directly related to the stiffness of the structure. The presence of a crack reduces the stiffness and consequently the natural frequencies. The additional surfaces created by new cracks tend to increase the damping ratios. A considerable amount of papers has been published to relate the change in modal parameters to the damage in a structure. For example, Admes *et al.* (1975) have used the change in natural frequencies to detect damage in composite materials. The same concept was applied to offshore structures (Loland and Dodds 1976, Vandiver 1975). Pandey *et al.* (1991) have proposed to use the change in curvature mode

† Lecturer in Solid Mechanics & Design
‡ Professor

shapes to localize damage. Nauerz and Fritzen (1996) have introduced a method for localization of faults based on power spectral densities.

The above technique is called "the response based approach" since the response data are directly related to damage. Another frequently used method known as "the model based approach" (Ahmadian *et al.* 1996, Nake and Cemple 1991, Hajela and Soeiro 1990, Zimmerman and Kaouk 1994) has been proposed to detect damage based on updating certain parameters to get perfect agreement between the experimental measured modal parameters and an initial finite element model. The updated parameters can be used afterwards to evaluate damage and identify its location. An excellent textbook discussing the updating techniques and their applications is due to Friswell and Mottershead (1995).

Before comparing two sets of dynamic parameters to detect damage, the effect of excitation type should be taken into consideration. If the excitation system for both tests is not the same, one should be known the influence of excitation system on the dynamic parameters of the underlined structure.

Dynamic tests can be subdivided into forced vibration and ambient vibration tests. In the first method, the structure is excited by artificial means such as shakers or drop weights. The disadvantage of this method is that the traffic has to be shut down for a rather long time, especially for large structures, e.g., long bridges. This can be a serious problem for intensively used bridges. In contrast, ambient vibration testing does not affect the traffic on the bridge because it uses the traffic as natural excitation. This method is cheaper than the first one because no extra costs are needed for exciting the structure. However, it requires relatively long records of response measurements. In the current measurements, two different excitations, namely impact weight and ambient vibrations due to the traffic over the bridge, are considered and the dynamic response of the bridge is measured.

Experimental modal analysis can be divided into frequency and time domain methods. Frequency domain analysis is mostly based on curve fitting of frequency response functions, obtained by dividing the Fast Fourier Transform (FFT) of the response and the force functions. The disadvantages of the FFT are: low frequency resolution, leakage, aliasing and contamination by noise. The data dependent system (DDS) method, originally developed by Pandit (1991), is a time domain identification method which doesn't require measurement of input forces. An autoregressive moving average vector model ARV(n) or ARMAV(n) is supposed to represent the measured response data. From the identified model, modal characteristics can be derived. In this paper, both techniques are used to derive the modal parameters: DDS method for the impact weight test and the coherence technique for the ambient vibration test.

In the following sections, first the autoregressive vector (ARV) model and the coherence technique are briefly reviewed. A brief description of the bridge and the dynamic tests are presented. Then, the finite element model is described. Finally, the results obtained from each test are compared and commented.

2. DDS method - ARV model

The simplest AR (1) model relating two successive observation of data is;

$$X_t = \varphi_1 X_{t-1} + a_t \tag{1}$$

where X_t and X_{t-1} are the observed output data, φ is the autoregressive parameter, a_t expresses the residual and t refers to the sequence index of observations. The part a_t arises because the dependence of X_t on X_{t-1} is not perfect. For an ideally deterministic system, the dependence would be perfect and a_t would be zero. Eq. (1) is called autoregressive model of order 1, AR(1). The order is 1 because X_t depends only on X_{t-1}. To be able to calculate X_t, we need initial values, i.e.;

$$X_t = X_o \ \text{ at } \ t = 0 \tag{2}$$

By a straightforward substitution, the solution of the differential Eq. (1) can be found as follows:

$$X_t = \varphi_1^t X_o + \sum_{j=0}^{t-1} \varphi_1^j a_{t-j} \tag{3}$$

The first term of Eq. (3) is called the deterministic part and the second term the stochastic part. Now, consider the case of simultaneous measurement of response data at p different locations ($\boldsymbol{X}_t$ (i), i=1, p). The vector $\boldsymbol{X}_t$ ($\boldsymbol{X}_t^T$=[X_{1t}, X_{2t}, ...X_{pt}]) can be written in the following form:

$$\boldsymbol{X}_t = \boldsymbol{\varphi}_1 \boldsymbol{X}_{t-1} + \boldsymbol{\varphi}_2 \boldsymbol{X}_{t-2} + \cdots\cdots + \boldsymbol{\varphi}_n \boldsymbol{X}_{t-n} + \boldsymbol{a}_t = \sum_{j=1}^{n} \boldsymbol{\varphi}_j \boldsymbol{X}_{t-j} + \boldsymbol{a} \tag{4}$$

Where $\boldsymbol{a}_t$=[$a_t(1)$ $a_t(2)$ ..... $a_t(p)$] and $\boldsymbol{\varphi}_j$ (j=1, n) are $p \times p$ matrices.
This model is known as a vector autoregressive model of order n, ARV(n).
The prediction error P_e (Pandit and Metha 1985) can be used to evaluate the accuracy of the model order n. The prediction error is defined as the ratio of the quadratic sum of the residual, $\boldsymbol{a}_t$, and the quadratic sum of the originally measured data (N points), i.e.;

$$P_{e_i} = \frac{N}{N-n} \frac{\sum_{t=n+1}^{N} [X_t(i) - \hat{X}_t(i)^2]}{\sum_{t=1}^{N} X_t^2(i)} \times 100\% \tag{5}$$

$$\hat{X}_t(i) = X_t(i) \qquad (t=1,\ n)$$

$$\hat{X}_t(i) = \sum_{j=1}^{n}\sum_{k=1}^{p} \boldsymbol{\varphi}_j(i,k) X_{t-j}(k) \qquad (t=n+1,\ N) \tag{6}$$

If $\boldsymbol{X}_o$ denotes the vector containing the initial values, one can obtain the modal decomposition for the ARV model analogous to Eq. (3) as follows:

$$\boldsymbol{X}_t = \boldsymbol{I}_p \boldsymbol{\Phi}^{t-n+1} \boldsymbol{X}_o^{(n-1)} + \sum_{j=0}^{t-n} \boldsymbol{G}_j \boldsymbol{a}_{t-j} \tag{7}$$

with $\boldsymbol{I}_p$=[**I 0 0 .... 0**], $\boldsymbol{I}$=$p \times p$ unit matrix, and

$$\boldsymbol{\Phi} = \begin{bmatrix} \boldsymbol{\varphi}_1 & \boldsymbol{\varphi}_2 & \cdots\cdots & \boldsymbol{\varphi}_{n+1} & \boldsymbol{\varphi}_n \\ \boldsymbol{I} & \boldsymbol{0} & \cdots\cdots & \boldsymbol{0} & \boldsymbol{0} \\ \boldsymbol{0} & \boldsymbol{I} & \cdots\cdots & \boldsymbol{0} & \boldsymbol{0} \\ \cdots & \cdots & \cdots & \cdots & \cdots \\ \boldsymbol{0} & \boldsymbol{0} & \cdots\cdots & \boldsymbol{I} & \boldsymbol{0} \end{bmatrix}$$

$\boldsymbol{X}_o^{(n-1)}$=[$\boldsymbol{X}_{o1}$ $\boldsymbol{X}_{o2}$ $\boldsymbol{X}_{o3}$ .... $\boldsymbol{X}_{o(np)}$]

and the Green's function $\boldsymbol{G}_j$ is

$$\boldsymbol{G}_j = \boldsymbol{I}_p \boldsymbol{\Phi}^j \boldsymbol{I}_p^T$$

If we assume that $\boldsymbol{\Phi}$ is diagonalizable, its spectral decomposition may be written as:

$$\boldsymbol{\Phi} = \boldsymbol{L}\boldsymbol{\lambda}\boldsymbol{L}^{-1} \tag{8}$$

where λ is the diagonal spectral matrix of Φ and L is the matrix of eigenvectors. The eigenvalues λ and the modal vectors $\boldsymbol{l}_i$ can be determined by solving the following autoregressive characteristic polynomial (Pandit 1991):

$$[\lambda_i^n \boldsymbol{I} - \lambda_i^{n+1}\boldsymbol{\varphi}_1 - \dots\dots\dots\dots \boldsymbol{\varphi}_n]\boldsymbol{l}_i = 0, \; i = 1, 2, \dots, n \times p \tag{9}$$

The eigenvalues of the continuous state mode μ are related to λ by the following equation:

$$\mu_i = \frac{1}{\Delta}\ln(\lambda_i) \tag{10}$$

where Δ is the sampling interval. The natural frequency ω_i and the damping ratio ξ_i can be found from the complex conjugate pairs of μ_i by:

$$\mu_i, \bar{\mu}_i = -\xi_i \omega_i \pm j\,\omega_i \sqrt{1-\xi_i^2} \tag{11}$$

After obtaining the solution, the important question arises how to select the modes and separate them from those arising from the measurement noise, computation, etc.... The first criteria for selection of the physical modes are the eigenfrequencies and the damping ratios. Knowledge of the frequency range of interest can be used to reject modes of lower or higher frequencies. Modes with high damping ratio may also be rejected as they damp out quickly. A second criterion is the average modal amplitude (AM) (Pandit 1991) which characterizes the strength of each mode in the deterministic part of the measured data X_t. Computational modes usually have small amplitude and can be rejected. The last criterion is the modal signal-to-noise ratio (MSN) which is defined as the ratio of AM to $\sqrt{\text{MV}}$, where MV is the summed up variance of the stochastic part of X_t. In addition to the above selection criteria, the results of a finite element simulations may also be used during the selection procedure of the relevant modes.

The ARV(n) model described in this section is implemented in a computer program DDS (De Roeck and Abdel Wahab 1996) developed at the department of Civil Engineering, Katholieke Universiteit te Leuven.

3. Coherence technique

Another frequently used technique to analyze ambient vibration test data is the coherence technique. In contrast to the DDS-methodology, the measured time signals are transformed in the frequency domain. Because the force cannot be measured, all response measurements are related to the response of one reference point. The frequency response functions (FRF) can then be evaluated with the classical FFT algorithms. Therefore, the FRF's are obtained as the ratio:

$$H_1 = \frac{G_{xy}}{G_{xx}} \tag{12}$$

where G_{xy} is the cross-spectrum between the output signals of the reference and the considered point, G_{xx} is the autospectrum. The symbols x and y denote the reference and the considered points, respectively.

The coherence function $R(f)$ is calculated as the ratio of the cross-spectrum to the individual autospectra, i.e.,

$$R(f)=\frac{|G_{xy}|^2}{G_{xx}\times G_{yy}} \tag{13}$$

The values of the coherence lie between 0 and 1. A high $R(f)$-value (>0.8) indicates a linear relationship between input and output signals. Therefore, the presence of a mode is indicated at this high coherence value. The value of the natural frequencies is calculated from the peaks on the cross-spectrum magnitude curve. The FRF's are combined to form the corresponding mode shapes which can be animated for visual identification.

4. Description of the bridge

The bridge B13 is located between the villages Vilvoorde and Melsbroek. The total length of the bridge is 102.37m divided over three spans (39.37m mid-span and 2×31.5 side-spans). B13 carries four traffic lanes and has a width of 26.0m and Fig. 1 shows a global overview of B13. The superstructure consists of 5 main girders in the longitudinal direction and 20 cross girders distributed over the three spans in the transversal direction. The deck is a concrete slab having a thickness of 0.18m, while the depth of the girders varies between 1.1m and 2.46m. Four abutments support the superstructure of the bridge. B13 is a skew-symmetric bridge but with a small skewness angle.

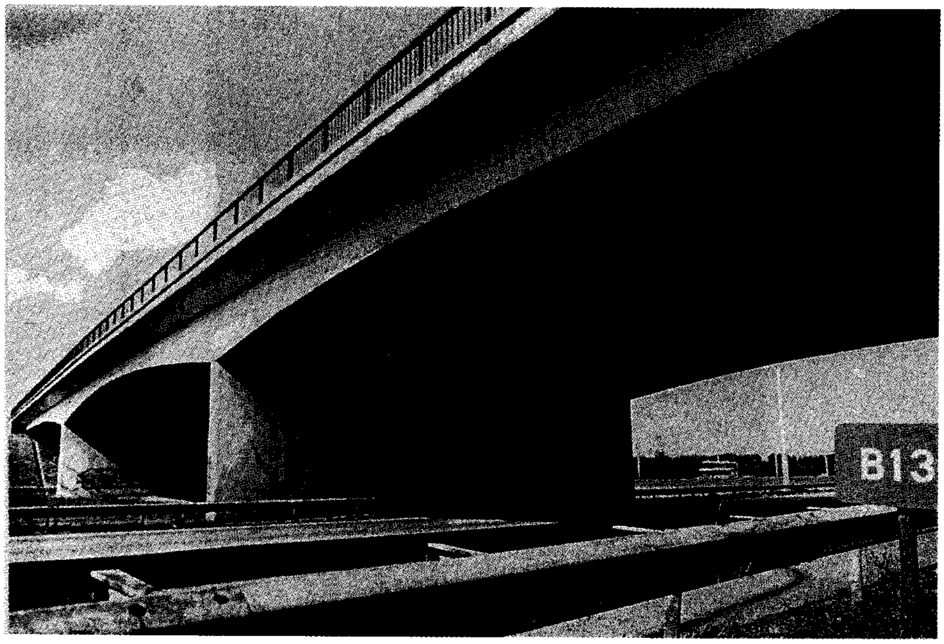

Fig. 1 Bridge B13

5. Description of the dynamic tests

5.1. Impact weight

Impact force was applied to the bridge using a weight of 120kg falling from a height of about 1.0m (see Fig. 2). The place of this weight was chosen according to the preliminary finite element results. The response of the bridge at selected points is measured in the vertical direction using accelerometers (PCB type 393A, 393A03, 393C, Schaevitz sch-x-o). Fig. 3 shows the experimental set up.

It was not possible to close the bridge due to its heavy traffic. Therefore, the impact weight and the accelerometers are placed on the sidewalk and the bicycle lane. It is worth mentioning that during the impact test measurement, we could not completely avoid the disturbance caused by the vehicles passing over the bridge because it was not possible to shut down the traffic. The response at 78 points (39 points x 2 sides) is registered as illustrated in Fig. 4. Each of the 10 series comprises response measurements in 8 points along the full bridge length. It should be noted that for both tests two reference points are considered to be able to combine the mode shapes afterwards.

For most bridges, the frequency range of interest is lying between 0 and 10Hz containing at least the first ten eigenfrequencies. The sampling frequency on site was chosen to be 500Hz. Afterwards, the data are resampled at 62.5Hz eliminating frequency components above 0.8 times

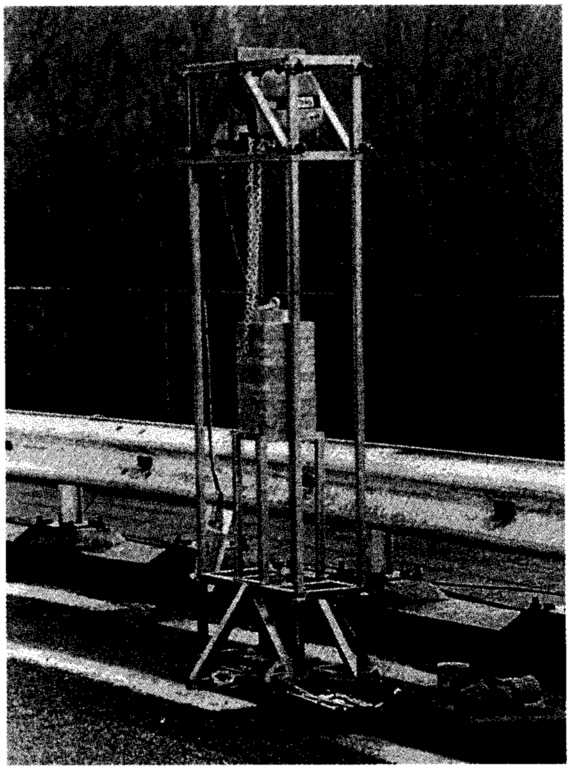

Fig. 2 Impact weight system

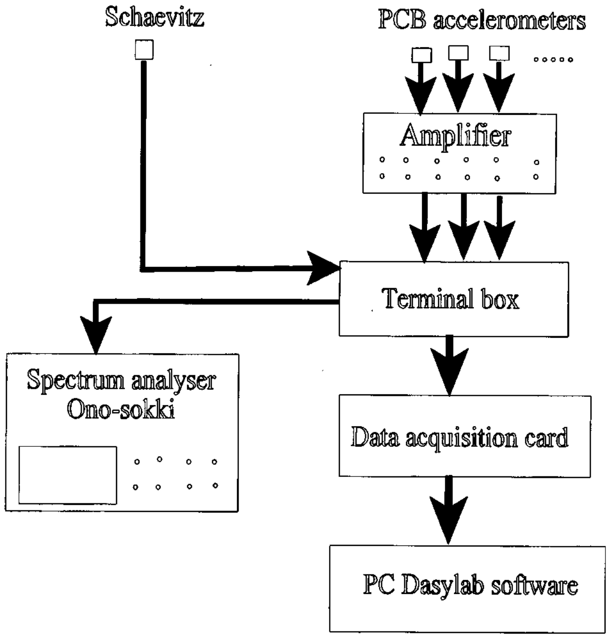

Fig. 3 Experimental set up

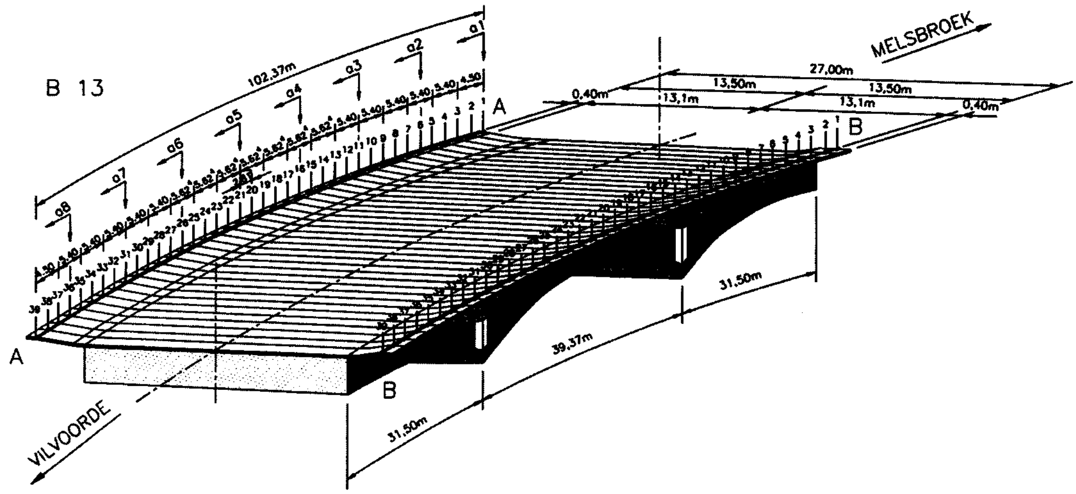

Fig. 4 Measurement locations

the Nyquist frequency (cutoff frequency of 25Hz).

5.2. Ambient vibration test

It is noteworthy that B13 has intensive traffic so that the traffic over this bridge is the main cause of vibrations. During a relatively long time interval, the vibrations of the bridge are registered at points mentioned under 5.1. The total acquisition time was 5 minutes at a sampling rate of 200Hz. Afterwards, the data were resampled to 25Hz resulting in a cutoff frequency of 10Hz.

6. Finite element model

The bridge is simulated using the finite element program ANSYS (1992). The whole bridge should be modelled to account for the skew-symmetric configurations. Four-noded shell elements with 6 degrees of freedom per node are used to model the two bridges. Fig. 5 shows the finite element mesh. The model contains 2230 nodes and 2870 elements. An extra mass is added at the deck of the bridges to account for the cover (asphalt, side walk, ...).

The finite element model is built before performing the dynamic tests. Its preliminary results are used to determine the location of the impact weight and that of the reference points. Afterwards, the model results are compared to the test results.

7. Results and comparisons

Since the main objective of this paper is to investigate the effect of the excitation type on the modal parameters of the bridge, it is important to check first the effect of the experimental errors due to environmental disturbance and electronic equipment. It should be noted that both

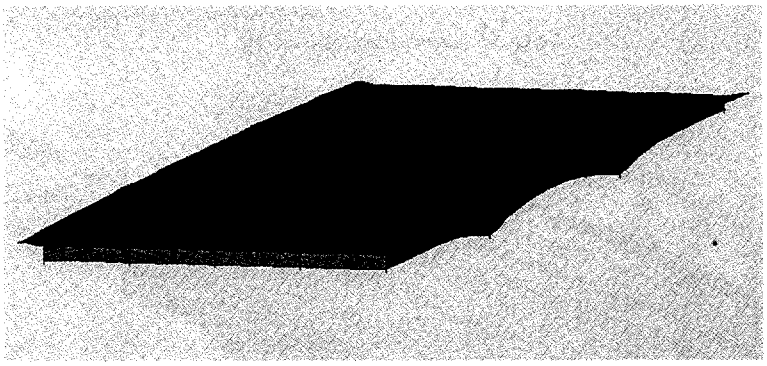

Fig. 5 F.E. mesh for B13-shell elements

Table 1 Comparison of natural frequencies for the different series-ambient test

	mode						
series	1	2	3	4	5	6	7
1	1.94	2.20	3.14	3.29	4.34	5.25	5.99
2	1.94	2.22	3.06	3.32	4.39	5.28	6.07
3	1.96	2.28	3.04	3.29	4.34	5.28	6.02
4	1.90	2.13	3.00	3.30	4.25	5.10	5.94
5	1.91	2.19	3.01	3.32	4.32	5.13	5.96
6	1.89	2.26	2.97	3.30	4.27	5.12	5.91
7	1.89	2.13	2.89	3.28	4.22	5.29	5.95
8	1.88	2.15	3.19	3.49	4.35	5.47	6.17
9	1.90	2.08	2.87	3.36	4.35	5.28	6.15
10	1.89	2.13	3.07	3.39	4.44	5.39	6.01
mean	1.91	2.18	3.02	3.33	4.33	5.26	6.02
St. Dev.	0.028	0.064	0.10	0.065	0.065	0.12	0.088

Table 2 Comparison of damping ratios (%) for the different series-ambient test

	mode						
series	1	2	3	4	5	6	7
1	2.32	4.34	3.16	2.48	2.04	2.35	1.86
2	2.95	3.20	3.81	1.83	2.10	2.31	1.83
3	3.28	4.58	2.12	2.01	1.56	0.92	2.05
4	3.65	6.13	1.97	1.95	1.67	1.56	1.52
5	2.63	2.14	2.71	1.67	1.89	5.37	1.78
6	2.94	2.00	0.70	3.42	0.57	0.40	2.94
7	2.30	5.79	1.80	2.65	2.55	1.91	2.34
8	1.94	1.13	1.63	3.24	2.24	2.25	1.97
9	1.92	1.17	1.03	0.88	1.96	0.79	0.73
10	9.40	9.46	1.86	0.61	1.13	1.68	5.50
mean	3.33	3.99	2.08	2.07	1.77	1.95	1.99
St. Dev.	2.20	2.63	0.93	0.91	0.57	1.37	1.38

measurements (impact and ambient tests) were carried out on the same day (under the same environmental condition). Therefore, minor influence is expected due to environmental condition. In order to check the experimental errors due to electronic equipment, the natural frequencies and damping ratios are extracted from each measurement series (in total 10 series were considered, see section 5) for the ambient test and are summarised in Tables 1 and 2 for the first seven vertical modes. The mean values and the standard deviations are given in the last two rows in Tables 1 and 2. Up to 2% variation in some eigenfrequencies can be observed. Obviously, the variation in damping ratios is much higher than that in eigenfrequencies.

Table 3 compares the natural frequencies obtained from the two measurements. In the fourth column of Table 3, the percentage difference between columns 2 and 3 is given. In the last column, the natural frequencies obtained from the finite element simulation are presented for convenience. In general the measured results are in good agreement with the numerical ones. The percentage difference in natural frequencies between the two tests is less than 1% for most of the modes. The changes in frequencies due to damage are expected to be higher than 1%. For example, it was found in Peeters *et al.* (1996) that for damaged concrete beam the natural frequencies changed by 10~18%. Therefore, the effect of excitation type on the frequencies will not significantly influence the non-destructive damage detection procedures. The damping ratios

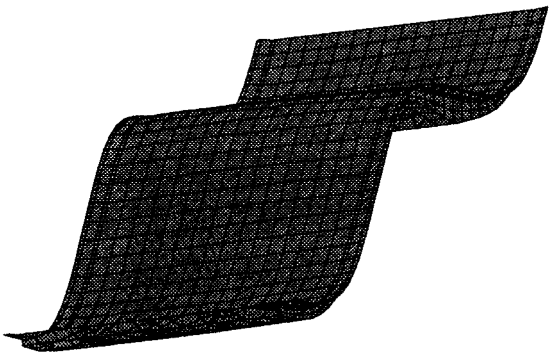

Fig. 6 mode 1-B13-F.E. results

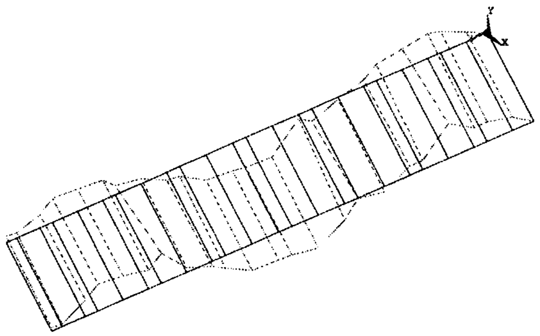

Fig. 7 model 1-B13-impact test

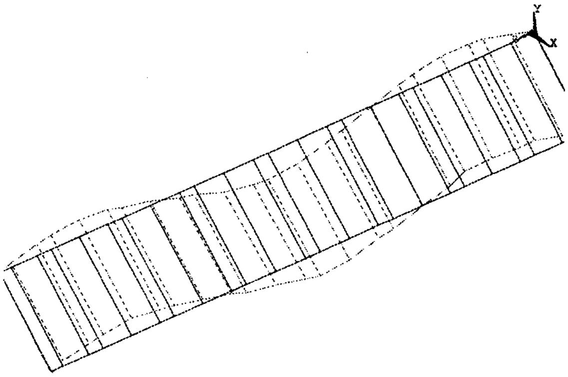

Fig. 8 mode 1-B13-ambient test

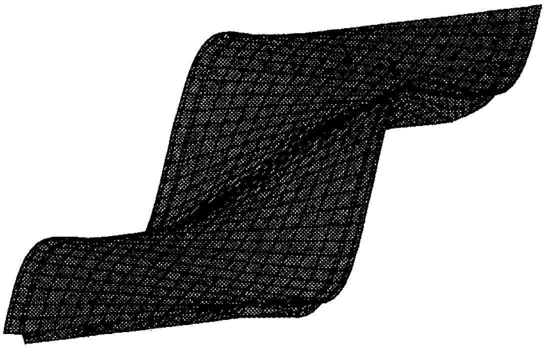

Fig. 9 mode 2-B13-F.E. results

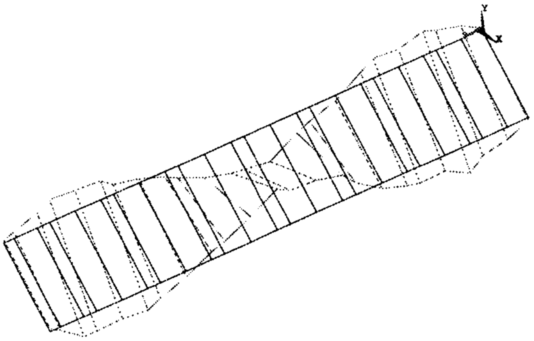

Fig. 10 mode 2-B13-impact test

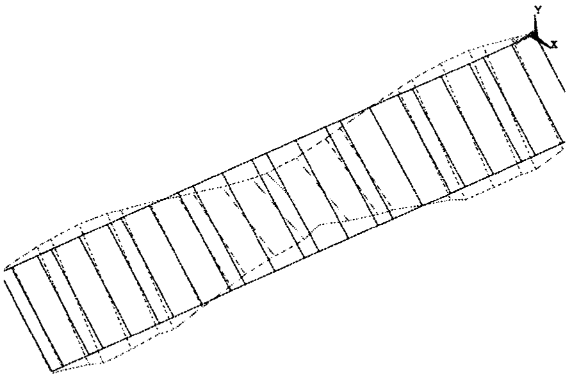

Fig. 11 mode 2-B13-ambient test

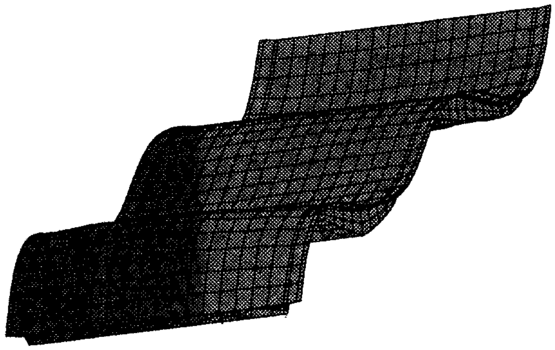

Fig. 12 mode 3-B13-F.E. results

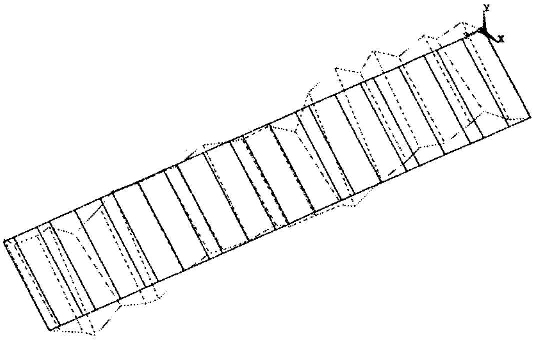

Fig. 13 mode 3-B13-impact test

obtained from both measurements are summarized in Table 4. Because the damping ratios are normally less accurate determined and depend on the data processing technique, a concrete conclusion can not be drawn from Table 4.

The first four mode shapes obtained from the finite element analysis, the impact test and the ambient test are compared in Figs. 6 to 17. The ambient test gives smoother mode shapes than the impact test. This could be due to some disturbance caused by the traffic over the bridge during the impact test measurement as mentioned before. A comparison between the measured and the

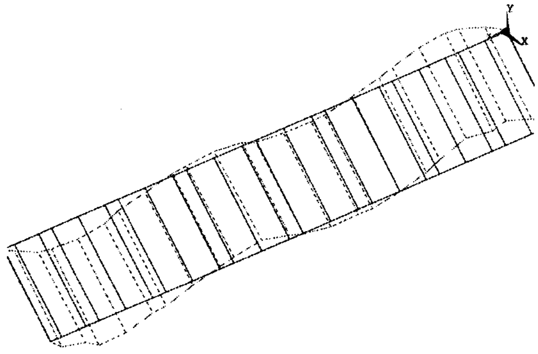

Fig. 14 mode 3-B13-ambient test

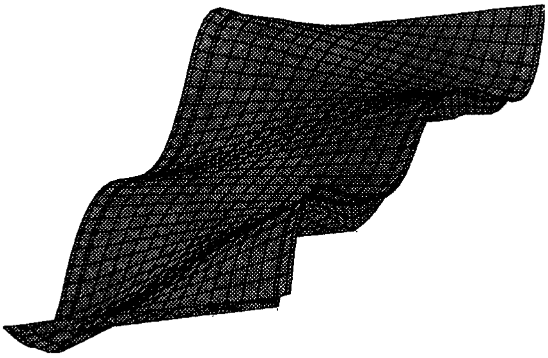

Fig. 15 mode 4-B13-F.E. results

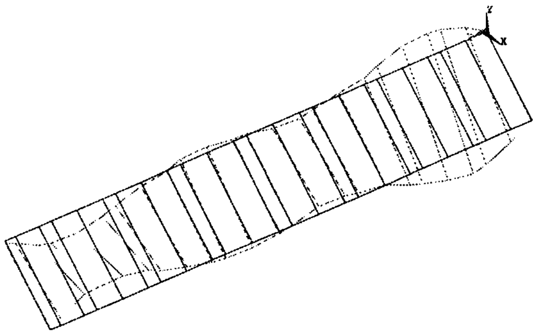

Fig. 16 mode 4-B13-impact test

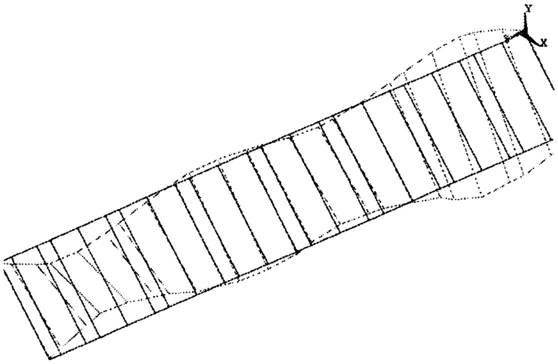

Fig. 17 mode 4-B13-ambient test

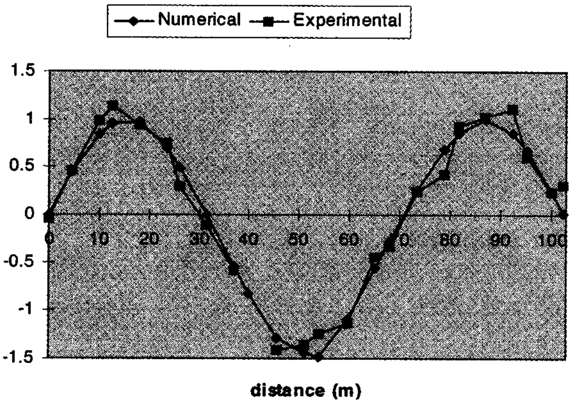

Fig. 18 mode 1-side Antwerpen-impact test

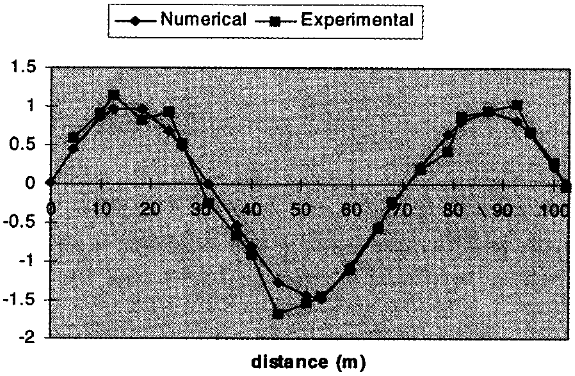

Fig. 19 mode 2-side Antwerpen-impact test

computed amplitudes is shown in Figs. 18 to 23 for modes 1, 2 and 4. It should be noted that the measured mode shapes are in general less accurate than the natural frequencies. Up to 20% measurement error in the model shapes may expected due to the environmental disturbance (Friswell and Mottershead 1995).

To evaluate the correlation between the computed and the measured mode shapes, the 'Modal Assurance Criterion' is calculated. The MAC-value is a correlation factor for each pair of analytical and experimental mode shapes. It is defined as Allemang and Brown (1982):

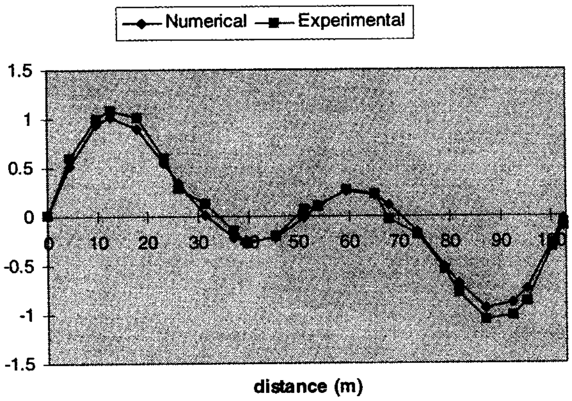

Fig. 20 mode 4-side Antwerpen-impact test

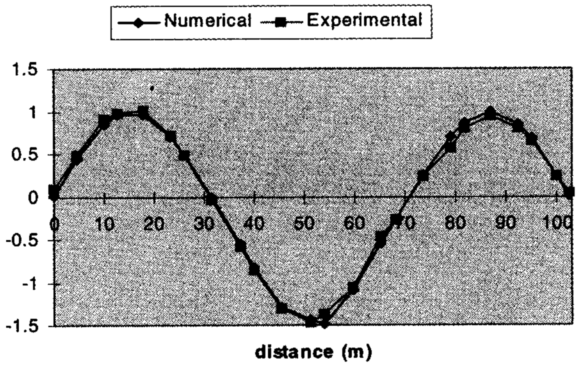

Fig. 21 mode 1-side Anetwepen-ambient test

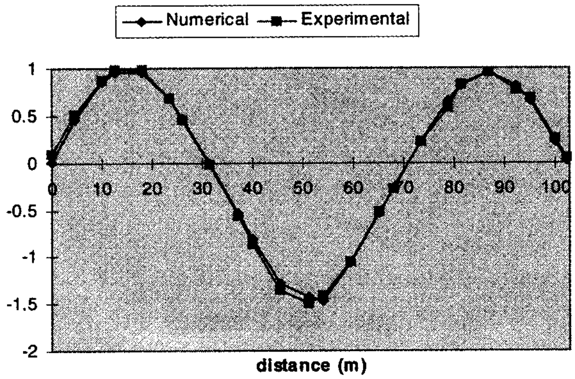

Fig. 22 mode 2-side Antwerpen-ambient test

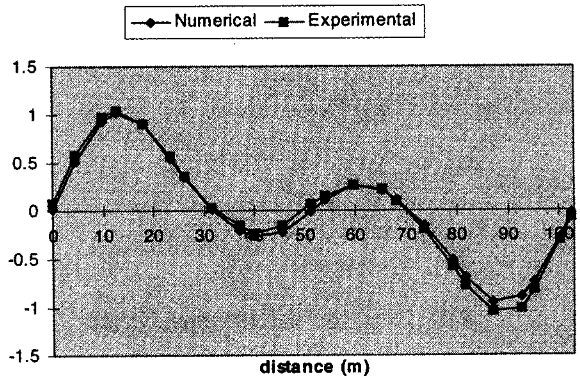

Fig. 23 mode 4-side Antwerpen-ambient test

$$\mathrm{MAC}(i,j)=\frac{|\Psi_i^* \; \Psi_j|}{\sqrt{\Psi_i^* \; \Psi_i}\sqrt{\Psi_j^* \; \Psi_j}} \tag{14}$$

Where Ψ is an 'eigenvector en * denotes i's complex conjugate.

De MAC-value always lies between 0 and 1. A MAC-value of 1 indicates excellent correlation, while a MAC-value of 0 indicates that the modes do not show any correlation. The diagonal of

Table 3 Comparison of natural frequencies-impact and ambient tests

Mode	Impact	Ambient	%difference between columns 2 and 3	F.E.M.
1	1.915	1.929	0.7	1.96
2	2.2	2.22	0.9	2.27
3	2.98	3.039	1.9	3.05
4	3.32	3.305	0.4	3.41
5	4.32	4.318	0.5	4.44
6	5.24	5.19	0.96	5.73
7	6.06	5.98	1.3	6.39

Table 4 Comparison of damping ratios (%)-impact and ambient test

Mode	1	2	3	4	5	6	7
Impact	3.59	3.7	3.64	1.19	2.01	2.9	2.1
Ambient	2.97	3.74	2.42	2.22	1.64	2.16	1.56

Table 5 MAC-matrix-B13-impact test

0.9725	0.0458	0.11514	0.04911	0.3378	0.01956
0.0097	0.9863	0.0521	0.0374	0.3047	0.0425
0.05159	0.0165	0.7994	0.0663	0.0270	0.9394
0.0877	0.01336	0.0708	0.99173	0.0602	0.0076
0.0145	0.0085	0.0590	0.0047	0.7868	0.1402
0.0470	0.0288	0.7981	0.0435	0.0180	0.9470

Table 6 MAC-matrix-B13-ambient test

0.9918	0.0792	0.0147	0.0690	0.0763	0.0649
0.0781	0.9896	0.02798	0.0317	0.0152	0.0481
0.0165	0.0178	0.9910	0.0616	0.0790	0.9025
0.0452	0.0034	0.0143	0.9909	0.0463	0.0590
0.0107	0.0236	0.0455	0.0088	0.9768	0.2338
0.0200	0.0292	0.9909	0.0386	0.0854	0.9110

the matrix MAC(i,j) should have a high value (>0.8) for good correlation. The MAC-matrix is calculated for the first six modes and is presented in Tables 3 and 4 for the impact test and the ambient test, respectively.

From these Tables it is evident that the correlation of the ambient test is better than that of the impact test. The off-diagonal elements (6,3) and (3,6) of the MAC-matrices are not close to zero. This means that those two modes have some similarities. In fact, mode 3 and 6 have the same global mode shape, but mode 6 has a bending form in the transverse direction. Because we have measured the response of points only on the sides of the bridge's cross section and not in the middle, the MAC-values (6,3) and (3,6) does not consider the mode form in the transverse direction. Therefore, those values are not considered to be relevant.

8. Conclusions

The influence of excitation type on the dynamic system parameters of a highway prestressed concrete bridge is investigated. Dynamic tests were performed on bridge B13 crossing the E19 highway in Belgium using two different excitations, impact weight and ambient conditions. Time domain and frequency domain techniques was used to extract the dynamic parameters from the recorded data. Finite element model was constructed to support and validate the dynamic measurements. It is shown that the percentage difference between the natural frequencies measured using impact weight and ambient vibration is less than 1% for most of the modes. Because the changes in the natural frequencies due to damage are likely to be of this order, it is important to take into account the effect of excitation type before using the modal parameters to evaluate damage.

Acknowledgements

This research work is a part of the research project IWT 950173 supported by the Flemish Government Institute IWT.

References

Adams, R.D., Walton, D. Flitcroft, J.E. and Short, D. (1975), "Vibration testing as a nondestructive test tool for composite materials", *Composite Reliability, ASTM STP* **580**, 159-175, Philadelphia: American Society for Testing and Materials.

Loland, O. and Dodds, C.J. (1976), "Experiences in developing and operating integrity monitoring system in north sea", *Proc. Proceedings of the 8th Annual Offshore Technology conference*, **2**, 331-3319, OTC paper n 2551.

Vandiver, J.K. (1975), "Detection of structural failure on fixed platforms by measurements of dynamic response", *Proceedings of the 7th Annual Offshore Technology Conference 2*, 243-252, OTC, paper n° 2267.

Pandey, A.K., Biswas, M. and Samman, M.M. (1991), "Damage detection from changes in curvature mode shapes", *Journal of Sound and Vibration*, **145**(2), 312-332.

Nauerz, A. and Fritzen, C.P. (1996), "Error localization using power spectral densities" The *21th International Seminar on Modal Analysis (ISMA 21)*, Noise and Vibration Engineering. 973-982.

Ahmadian, H., Mottershead, J.E. and Friswell, M.I. (1996), "Damage detection from substructure modes", *The 21th International Seminar on Modal Analysis (ISMA 21)*, Noise and Vibration Engineering, 983-991.

Nake, H.G. and Cemple, C. (1991), "Fault detection and localization in structures: A discussion", *Mechanical Systems and Signal Processing*, 345-359.

Hajela, P. and Soeiro, F.J. (1990), "Structural damage detection based on static and modal analysis", *AIAA Journal,* **28**(6), 1110-1115,

Zimmerman, D.C. and Kaouk, M. (1994), "Structural damage detection using a minimum rank updating theory", *Journal of Vibration and Acoustics*, **116**, 222-231.

Friswell, M.I. and Mottershead, J.E. (1995), *Finite Element Model Updating in Structural Dynamics*, KLUWER Academic Publisher, Dordrechts, The Netherlands.

Pandit, S. (1991), *Modal and Spectrum Analysis: Data Dependent System in State Space*, John Wiley & Sons.

Pandit, S. and Metha, N.P. (1985), "Data dependent systems approach to modal analysis via state space", *ASME* paper n° 85 -WA/DSC-1.

De Roeck, G., Abdel Wahab, M. and Claesen, W. (1996), "System identification using the data dependent system method", Version 1.1. Department of Civil Engineering, Katholieke Universiteit te Leuven.

ANSYS, revision 5.3, (1992), Swanson Analysis Systems.

Peeters, B., Abdel Wahab, M., De Roeck, G., De Visscher, J., De Wilde, W.P., Ndambi, J.-M. and Vantomme, J., (1996), "Evaluation of structural damage by system identification", The *21th International Seminar on Modal Analysis (ISMA 21)*, Noise and Vibration Engineering, 1349-1362.

Allemang, R.J. and Brown, D.L. (1982), "A correlation coefficient for modal vector analysis", *1st International Modal Analysis Conference,* Orlando, Florida, 110-116.